Bioorganic & Medicinal Chemistry Letters 20 (2010) 4607–4610

Contents lists available at ScienceDirect

Bioorganic & Medicinal Chemistry Letters

journal homepage: www.elsevier.com/locate/bmcl

Addressing PXR liabilities of phthalazine-based hedgehog/smoothened antagonists using novel pyridopyridazines

Jacob A. Kaizerman, Wade Aaron, Songzhu An, Richard Austin, Matt Brown, Angela Chong, Tom Huang, Randall Hungate, Ben Jiang, Michael G. Johnson, Gary Lee, Brian S. Lucas, Jessica Orf, Minqing Rong, Maria M. Toteva, Dineli Wickramasinghe, Guifen Xu, Qiuping Ye, Wendy Zhong, Dustin L. McMinn *

Amgen, Inc., 1120 Veterans Boulevard, South San Francisco, CA 94080, USA

ARTICLE INFO

Article history:
Received 27 April 2010
Accepted 1 June 2010
Available online 8 June 2010

Keywords:
Hedgehog
Smoothened
Hh
SMO
Cancer
Oncology

ABSTRACT

Pyridopyridazine antagonists of the hedgehog signaling pathway are described. Designed to optimize our previously described phthalazine smoothened antagonists, a representative compound eliminates a PXR liability while retaining potency and in vitro metabolic stability. Moreover, the compound has improved efficacy in a hedgehog/smoothened signaling mouse pharmacodynamic model.

The hedgehog (Hh) signaling pathway regulates cell growth and differentiation in developing tissues.[1] Deregulation of this pathway has been linked to tumorigenesis in a variety of cancers[2,3] and is clearly implicated in development of basal cell carcinoma[4] and medulloblastoma.[5] Smoothened (Smo), a seven-transmembrane cell surface receptor, transduces Hh signaling and is responsible for activation of the Gli family of zinc finger transcription factors. Once activated, Gli transcription factors drive the expression of genes involved with cell proliferation and, when deregulated, cancer (cyclins and CDK's, BCL2 (survival) and Snail (metastasis), as well as Gli1). In normal tissues, Smo is prevented from activating Gli transcription factors by the action of the 12-transmembrane protein Patched (Ptch). Upon binding to Hh or when plagued by inactivating mutations, Ptch no longer inhibits Smo, thus allowing the effector Smo to drive unregulated expression of Hh target genes. The promise of treating cancer via antagonism of Smo and disruption of aberrant Hh signaling has driven considerable recent efforts in our labs[6] and on the part of the wider pharmaceutical industry.[7]

We have recently described a series of 4-(4-phenylphthalazine-1-yl)piperazine amide-based inhibitors of Smo.[8,9] Structural optimization led to **1**, a compound which proved highly potent against mouse (mSMO) and human (hSMO) forms of Smo (Fig. 1).[10] Moreover, **1** showed efficacy in established pharmacodynamic and tumor models representative of Hh pathway disruption.[11] Further evaluation of **1** and related compounds revealed a pregnane X receptor (PXR) activation liability, thus presenting for this series of compounds the potential for transactivation of a variety of drug metabolizing enzymes and subsequent drug–drug interactions. The cancer indication presents an ever-increasing polypharmic population and thus encourages the development of oncology drugs known to avoid erratic drug metabolism and the associated potential for therapeutic failure.[12] We describe here our efforts to eradicate PXR liabilities from our Smo antagonists while preserving potency and pharmacodynamic efficacy.

From our previously submitted work, we disclosed that appropriate substitution of the 4-phenyl group was generally well tolerated and in some cases led to improved in vitro and in vivo metabolic stability. For this reason, we initially sought to evaluate PXR activation as it relates to modification at this region of the molecule. Synthesis of compounds **1–7, 12, 14–16, 21** and **22** have

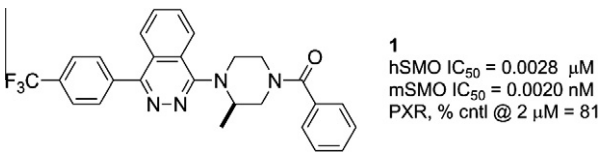

Figure 1. Smoothened antagonist.

* Corresponding author.
E-mail address: dmcminn@amgen.com (D.L. McMinn).

0960-894X/$ - see front matter © 2010 Elsevier Ltd. All rights reserved.
doi:10.1016/j.bmcl.2010.06.006

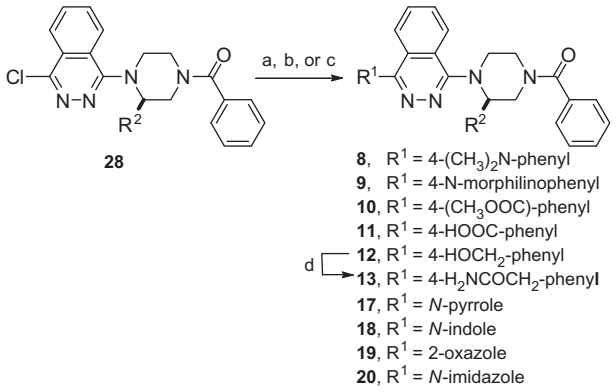

Scheme 1. (a) R^1-$B(OH)_2$, $Pd(PPh_3)_4$, Na_2CO_3, toluene, 100 °C, 71–97%; (b) pyrrole, indole, or imidazole, CuI, K_3PO_4, *trans*-1,2-diaminocyclohexane, dioxane, 110 °C, 14–50%; (c) 2-(tri-*N*-butylstannyl)oxazole, $Pd[P(t\text{-}Bu)_3]_2$, CsF, dioxane, 25%; (d) 2,2,2-trichloroacetyl isocyanate, neutral alumina (Brockmann II), chloroform, 99%.

been described.[8,13] Compounds **8–12** and **17–20** were derived from our previously described intermediate **28** (Scheme 1) utilizing Suzuki (**8–12**), Buchwald copper mediated N-heteroarylation[15] (**17, 18,** and **20**) or Stille couplings (**19**). Conversion of the benzyl alcohol **12** to the primary carbamate **13** was achieved using 2,2,2-trichloroacetyl isocyanate and subsequent alumina hydrolysis.

With the exception of **11**, substitutions on the 4-phenyl ring rendering increased calculated log *D* coefficients led to increased PXR activation (**1** vs **2**, **3** vs **4**, and **5** vs **6**, Table 1). In contrast, compounds with less lipophilic groups at the *para*-position of the 4-phenyl ring exhibited reduced PXR activation (**7**–**13**). Compounds **7–9** failed to combine minimized PXR potential with sufficient biochemical potency, while compounds **10** and **11**, although quite potent, showed compromised in vitro metabolic stability in rat or human liver microsome homogenates. Compounds **12** and **13** exhibited potency and in vitro metabolic stability comparable to the parent compound **1**. For these compounds, though, there was a disconnect between in vitro metabolic stability in rat liver microsomal homogenates and their observed moderate to high clearance in vivo (Table 3). Substituting the phenyl group with heteroaryl functionality containing one heteroatom resulted in compounds with significantly compromised potency (**14**–**16**) or decreased in vitro metabolic stability (**17** and **18**). Support for a hydrophobicity-driven PXR transactivation hypothesis in this structural class was corroborated by comparison of PXR activation by the N-linked pyrrole **17** to the more hydrophobic N-linked indole **18** (12% vs 74%, respectively). Heteroaryl groups at the 4-position containing more than two heteroatoms showed low PXR potential and minimal in vitro metabolic turnover, albeit at the cost of target potency (**19–22**).

Having shown that increasing polarity of pendant features could potentially mitigate PXR transactivation, we hypothesized that increased polarity in the upper ring of the phthalazine core would also provide compounds with low PXR potential. Moreover, such new scaffolds may provide an opportunity to address the PXR liability while preserving potency and metabolic stability. We chose to test this hypothesis by incorporating single nitrogen at each position of the benzo-portion of the phthalazine core, thus rendering pyridopyridazines **23–26** (Table 2).

Syntheses of pyridopyridazines are outlined in Schemes 2–4. Preparation of 5-((2*R*)-2-methyl-4-(phenylcarbonyl)-1-piperazinyl)-8-phenylpyrido[3,2-*d*]pyridazine **23** went though the 5,8-dichloropyrido[2,3-*d*]pyridazine intermediate **31** which was prepared by sequential treatment of 2,3-pyridinedicarboxylic anhydride with hydrazine and $POCl_3$ (Scheme 2). Regioselective nucleophilic

Table 1
Phthalazine-based Smoothened inhibitors

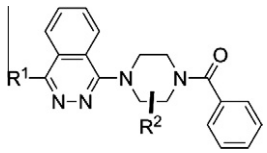

Compd	R^1	R^2	hSMO IC_{50} (μM)[a]	PXR, % activ. at 2 μM[b]	log *D* (pH 7.4)[c]	%TO RLM[d]	%TO HLM[d]
1	4-(Trifluoromethyl)phenyl	3-*R*-methyl	0.0028	81	3.74	11	13
2	Phenyl	3-*R*-methyl	0.0022	30	2.29	12	44
3	3,4-Dichlorophenyl	H	0.017	48	3.34	13	31
4	Phenyl	H	0.019	12	1.8	39	19
5	F-phenyl	2-*S*-methyl	0.012	61	2.49	21	<10
6	Phenyl	2-*S*-methyl	0.0053	32	2.29	<10	<10
7	4-NH_2CO-phenyl	3-*R*-methyl	0.019	5.9	1.12	<10	<10
8	4-*N*-Morpholinophenyl	3-*R*-methyl	0.021	6.6	0.95	28	19
9	4-HOOC-phenyl	3-*R*-methyl	>1	2.7	0.08	<10	<10
10	4-$(CH_3)_2N$-phenyl	3-*R*-methyl	0.0053	17	1.97	82	59
11	4-(CH_3OCO)-phenyl	3-*R*-methyl	0.0033	6.1	2.59	>95	>95
12	4-$HOCH_2$-phenyl	3-*R*-methyl	0.0027	3	1.3	15	14
13	4-H_2NCOCH_2-phenyl	3-*R*-methyl	0.0048	2.7	1.52	10	10
14	4-Pyridyl	3-*R*-methyl	0.025	25	1.46	36	11
15	3-Pyridyl	3-*R*-methyl	0.079	23	1.49	16	19
16	2-Pyridyl	3-*R*-methyl	0.057	16	1.56	17	12
17	*N*-Pyrrolyl	3-*R*-methyl	0.0087	12	2.02	63	54
18	*N*-Indolyl	3-*R*-methyl	0.0080	74	2.99	72	55
19	2-Oxazolyl	3-*R*-methyl	>1	7.8	1.61	22	<10
20	*N*-Imidazolyl	3-*R*-methyl	>1	3.7	0.72	16	<10
21	2-Pyridazinyl	3-*R*-methyl	>1	5.4	0.04	<10	<10
22	5-Pyrimidinyl	3-*R*-methyl	>1	7.1	0.52	<10	<10

[a] Values are the average of a minimum of three measurements.
[b] Rifampin used as control.[14]
[c] ACD based calculation.
[d] Percent turnover within 30 min in liver microsome homogenates.

Table 2
Pyridopyridazine-based smoothened inhibitors

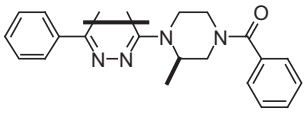

Compd	Ring	hSMO IC_{50} (μM)	PXR, % activ. at 2 μM[a]	%TO HLM[b]
23		0.066	4.1	13
24		0.016	5.7	56
25		0.012	7.5	30
26		0.0058	4.9	13

[c] Percent turnover within 30 min in liver microsome homogenates.
[a] Values are the average of a minimum of three measurements.
[b] Rifampin used as control.

heteroaromatic substitution with (*R*)-1-benzoyl-3-methylpiperazine provided **32** which served as the substrate for a final Suzuki coupling. Alternatively, 8-((2*R*)-2-methyl-4-(phenylcarbonyl)-1-piperazinyl)-5-phenylpyrido[2,3-*d*]pyridazine synthesis commenced with conversion of 3-benzoylpicolinic acid **33** to the 8(7*H*)-pyrido[2,3-*d*]pyridazinone **34** (Scheme 3). Chloride synthesis, substitution, deprotection of intermediate **36**, and benzoylation provided **24**. Synthesis of the common intermediate **39** for preparation of 1-((2*R*)-2-methyl-4-(phenylcarbonyl)-1-piperazinyl)-4-phenylpyrido[4,3-*d*]pyridazine and 4-((2*R*)-2-methyl-4-(phenylcarbonyl)-1-piperazinyl)-1-phenylpyrido[3,4-*d*]pyridazine followed that of **31** (Scheme 4). Predictive electronics of the 1,4-dichloropyrido[3,4-*d*]pyridazine system afforded significantly higher isolated substitution yields for **41** than for **40**. Suzuki coupling with the appropriate boronic acid was followed by removal of Boc protection and benzoylation to provide **25** and **26**. Compounds **23**–**26** successfully reduced PXR activation to well below the levels of **1**. The 4-((2*R*)-2-methyl-4-(phenylcarbonyl)-1-piperazin-yl)-1-phenyl-pyrido[3,4-*d*]pyridazine compound, **26**, proved to be the optimal regioisomer addressing in concert potency, in vitro metabolic stability, and PXR activation. To assess the capacity for this scaffold to reduce PXR activation, we reinstalled the trifluoromethyl feature at the *para*-position of the 1-phenyl group (**27**, Fig. 2). To our satisfaction,

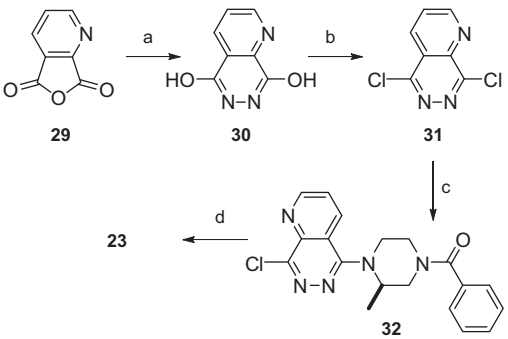

Scheme 2. (a) Acetic acid, hydrazine, 100 °C, 68%; (b) $POCl_3$, pyridine, 110 °C, 38%; (c) (*R*)-(3-methylpiperazin-l-yl)(phenyl)methanone, melt, 44%; (d) $PhB(OH)_2$, $Pd(PPh_3)_4$, Na_2CO_3, toluene, 100 °C, 77%.

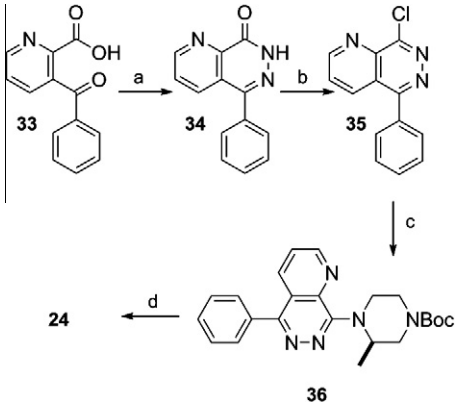

Scheme 3. (a) Hydrazine, ethanol, reflux, 71%; acetic acid, hydrazine, 100 °C, 68%; (b) $POCl_3$, pyridine, 110 °C, 80%; (c) (*R*)-*tert*-butyl 3-methylpiperazine-l-carboxylate, 130 °C melt, 52%; (d) TFA, CH_2C1_2, 77%; (e) benzoyl chloride, TEA, CH_2C1_2, 84%.

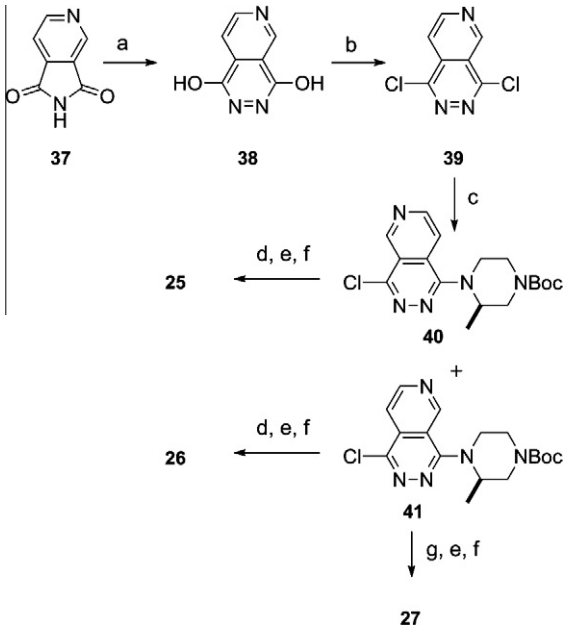

Scheme 4. (a) NH_2NH_2, ethanol, H_2O, reflux, 99%; (b) $POCl_3$, Hünig's base, reflux, 67%; (c) (*R*)-*tert*-butyl 3-methylpiperazine-l-carboxylate, Hünig's base, NMP, 100 °C, 2% isolated yield for **40**, 62% isolated yield for **41**; (d) $PhB(OH)_2$, $Pd(PPh_3)_4$, Na_2CO_3, toluene, 100 °C, 99%; (e) TFA, CH_2C1_2, 99%; (f) benzoyl chloride, TEA, CH_2C1_2, 55–77%; (g) 4-$CF_3PhB(OH)_2$, $Pd(PPh_3)_4$, Na_2CO_3, toluene, 100 °C, 99%.

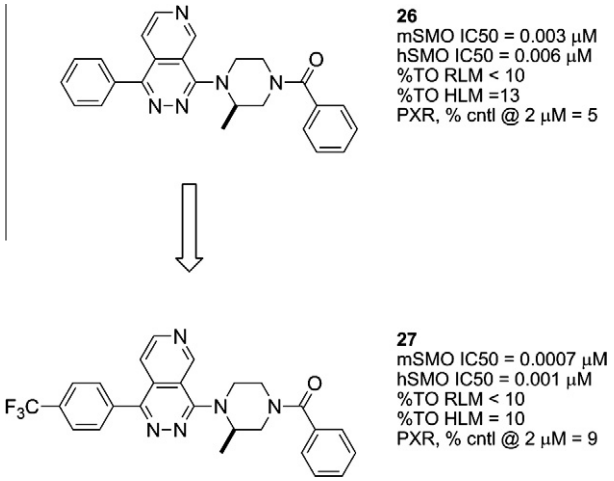

Figure 2. Compounds **26** and **27**.

Table 3
Rat and mouse pharmacokinetics for selected phthalazine and pyridopyridazine-based smoothened inhibitors[a]

Compd	Species	CL (iv, L/h/kg)	Vdss (L/kg)	AUC_{po} (μg h/L)	%F
1	Rat	0.41	5.1	1200	39
2	Rat	0.28	1.7	1800	15
12	Rat	5.7	1.8	BQL	nd
13	Rat	1.1	1.4	460	22
26	Rat	0.45	1.4	1600	35
27	Rat	0.46	3.5	3300	73
27	Mouse	0.64	2	3500	46

[a] Dosed iv 0.5 mg/kg, po 2 mg/kg.

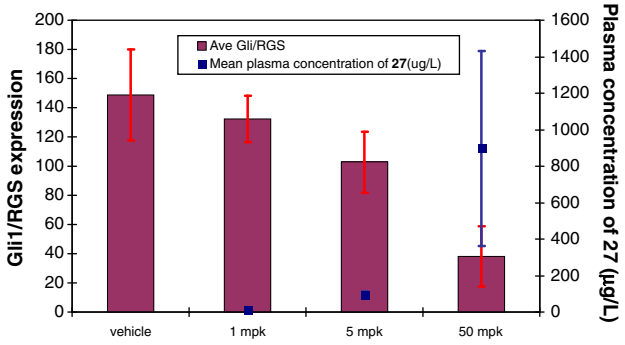

Figure 3. Reduction of Gli1 expression in skins of mice treated with **27**. Four animals per group, two samples per animal; 1 mg/kg, $\rho = 0.355$; 5 mg/kg, $\rho = 0.0011$; 50 mg/kg, $\rho < 0.0001$ (Dunnet's method).

not only was PXR activation suppressed, but potency in the human biochemical assay was improved sixfold relative to **26**. These qualities were augmented by impressive in vivo pharmacokinetic profiles in potential representative pharmacodynamic model species (Table 3). Compound **27** provided superior oral exposure relative to **26** in rats and exhibited low clearance and good oral bioavailability in the mouse. Finally, compounds **26** and **27**, as representatives of this class, showed excellent potency in the mouse, our species of choice for pharmacodynamic efficacy assessment.

Our pharmacodynamic model relies upon the known overexpression of Hh target genes in the depilated skin of mice.[10] The Hh signaling pathway is activated during the growth stage of the hair cycle resulting in up-regulation of target genes including Gli1. Skins of mice were depilated and, after 5 days, were harvested 6 h post-oral dosing with **27**. Gli1 expression was measured against reference genes. Figure 3 shows a dose dependent reduction of Gli1 expression was observed (approximate $EC_{50} = 0.46$ μM). This result constitutes an improvement over the performance of our previously reported compound **1** in this model ($EC_{50} = 2.0$ μM).[16,8]

In conclusion, pyridopyridazines described in this work constitute a novel class of SMO inhibitors capable of suppressing PXR transactivation, a potential liability seen for our previously reported potent phthalazine-based inhibitors. Compounds **26** and **27** of the 4-((2*R*)-2-methyl-4-(phenylcarbonyl)-1-piperazin-yl)-1-phenylpyrido[3,4-*d*]pyridazine regio-isomeric sub-class highlight our ability to redress PXR liabilities while maintaining potency and metabolic stability in vitro. Finally, compound **27** proved efficacious at disrupting Hh signaling in an in vivo pharmacodynamic model. These results merit our continued investigation of this structural class.

References and notes

1. Ingham, P. W.; McMahon, A. P. *Genes Dev.* **2001**, *15*, 3059.
2. Rubin, L. L.; de Sauvage, F. J. *Nat. Rev. Drug Discov.* **2006**, *5*, 1026.
3. Lum, L.; Beachy, P. A. *Science* **2004**, *304*, 1755.
4. Epstein, E. H. *Nat. Rev. Cancer* **2008**, *8*, 743.
5. Berman, D. M.; Karhadkar, S. S.; Hallahan, A. R.; Pritchard, J. I.; Eberhart, C. G.; Watkins, D. N.; Chen, J. K.; Cooper, M. K.; Taipale, J.; Olson, J. M.; Beachy, P. A. *Science* **2002**, *297*, 1559.
6. (a) Austin, R. J.; Kaizerman, J.; Lucas, B.; McMinn, D. L.; Powers, J. PCT Int. Appl. WO 2009/002469 A1, 2009.; (b) Kaizerman, J.; Lucas, B.; McMinn, D. L.; Zamboni, R. PCT Int. Appl. WO 2009/035568 A1, 2009.
7. (a) Miller-Moslin, K.; Peukert, S.; Jain, R. K.; McEwan, M. A.; Karki, R.; Llamas, L.; Yusuff, N.; He, F.; Li, Y.; Sun, Y.; Dai, M.; Perez, L.; Michael, W.; Sheng, T.; Lei, H.; Zhang, R.; Williams, J.; Bourret, A.; Ramamurthy, A.; Yuan, J.; Guo, R.; Matsumoto, M.; Vattay, A.; Maniara, W.; Amaral, A.; Dorsch, M.; Kelleher, J. F. *J. Med. Chem.* **2009**, *52*, 3954; Review of recent efforts in the field of Hh signaling regulation: (b) Mahindroo, N.; Punchihewa, C.; Fujii, N. *J. Med. Chem.* **2009**, *52*, 3829; (c) Peukert, S.; Jain, R. K.; Geisser, A.; Sun, Y.; Zhang, R.; Bourret, A.; Carlson, A.; DaSilva, J.; Ramamurthy, A.; Kelleher, J. F. *Bioorg. Med. Chem. Lett.* **2009**, *19*, 328; (d) Tremblay, M. R.; Nevalainen, M.; Nair, S. J.; Porter, J. R.; Castro, A. C.; Behnke, M. L.; Yu, L.-C.; Hagel, M.; White, K.; Faia, K.; Grenier, L.; Campbell, M. J.; Cushing, J.; Woodward, C. N.; Hoyt, J.; Foley, M. A.; Read, M. A.; Sydor, J.; Tong, J. K.; Palombella, V. J.; McGovern, K.; Adams, J. *J. Med. Chem.* **2008**, *51*, 6646; (e) Feldmann, G.; Fendrich, V.; McGovern, K.; Bedja, D.; Bisht, S.; Alvarez, H.; Koorstra, J.-B. M.; Habbe, N.; Karikari, C.; Mullendore, M.; Gabrielson, K. L.; Sharma, R. *Mol. Cancer Ther.* **2008**, *7*, 2725; (f) Brunton, S. A.; Stibbard, J. H. A.; Rubin, L. L.; Kruse, L. I.; Guichert, O. M.; Boyd, E. A.; Price, S. *J. Med. Chem.* **2008**, *51*, 1108; (g) Remsberg, J. R.; Lou, H.; Tarasov, S. G.; Dean, M.; Tarasova, N. I. *J. Med. Chem.* **2007**, *50*, 4534; (h) Rudin, C. M.; Hann, C. L.; Laterra, J.; Yauch, R. L.; Callahan, C. A.; Fu, L.; Holcomb, T.; Stinson, J.; Gould, S. E.; Coleman, B.; LoRusso, P. M.; Von Hoff, D. D.; de Sauvage, M. J.; Low, J. A. *NEJM* **2009**, *361*, 1173.
8. Lucas, B. S.; Aaron, W.; An, S.; Austin, R. J.; Brown, M.; Chan, H.; Chong, A.; Hungate, R.; Huang, T.; Jiang, B.; Johnson, M. G.; Kaizerman, J. A.; Lee, G.; McMinn, D. L.; Orf, J.; Powers, J. P.; Rong, M.; Toteva, M. M.; Uyeda, C.; Wickramasinghe, D.; Xu, G.; Ye, Q.; Zhong, W. *Bioorg. Med. Chem. Lett.* **2010**, *20*, 3618.
9. Inhibitors of the Hh pathway featuring a piperazine-substituted phthalazines have been described, Ref. 7a.
10. Biological methods: *IC_{50} assay for mouse Smo*: mouse smoothened activity was measured in vitro using a modified version of the method described.[11d] An oligonucleotide cassette with five consensus Gli1 binding sites was ligated into the luciferase reporter plasmid pGL4.16 (Promega, Madison, WI, USA). A stable clone of NIH-3T3 cells stably transfected with the Gli1-binding-site plasmid was used for the reporter assay. Compounds were incubated with cells for 15 h in the presence of Optimem medium (Invitrogen, Carlsbad, CA, USA) supplemented with 0.5% charcoal–dextran treated fetal bovine serum (HyClone) and 10 mM myristoylated mouse Shh protein (Williams et al., 1999). Luciferase activity was measured by addition of Bright-Glo (Promega) and reading on a luminometer. Compounds were tested in quadruplicate using a threefold dilution series.
IC_{50} assay for human SMO: HEPM cells were used to measure human SMO activity in vitro using a modified version of the method described by others [US Patent 6,613,798]. In 96 well tissue culture plates, compounds were incubated with HEPM cells in the presence of MEM media supplemented with 0.5% charcoal–dextran treated fetal bovine serum (HyClone) and 50 mM myristoylated mouse Shh protein (Williams et al. 1999). Twenty-four hours after the addition of compound and Shh, GLI expression was measured using a Quantigene assay (Affymetrix, Santa Clara, CA, USA).
Mouse skin pharmacodynamic model: Female NOD-Scid mice (Taconic, Hudson, NY, USA) aged 5–8 weeks were shaved on one side of the hind flank. Four days after shaving, mice were anesthetized and regrown hair was removed using hair removal wax strips. After 5 days, mice were dosed orally with compounds or vehicle. At specified time points after dosing, animals were sacrificed and the waxed regions of skin were excised and stored in RNALater solution (Ambion, Austin, TX, USA) at 4 °C. Skin samples were homogenized in Lysis buffer (Ambion) using a Tomtec Autogizer (Hamden, CT, USA); RNA was purified using an *mir*Vana miRNA Isolation Kit (Ambion). RNA was converted cDNA using reverse transcriptase prior to quantitative, real time PCR analysis (Applied Biosystems, Foster City, CA, USA). Gli1 expression was normalized to Rgs3 expression using the standard curve method.
11. (a) Paladini, S.; Qian, X.; Rubin *J. Invest. Dermatol.* **2005**, *125*, 638; (b) Williams, K. P.; Rayhorn, P.; Chi-Rosso, G.; Garber, E. A.; Strauch, K. L.; Horan, G. S. B.; Reilly, J. O.; Baker, D. P.; Taylor, F. R.; Koteliansky, V.; Pepinsky, R. B. *J. Cell Sci.* **1999**, *112*, 4405; (c) U.S. Patent 6,613,798.; (d) Chen, J. K.; Taipale, J.; Young, K. E.; Maiti, T.; Beachy, P. A. *PNAS* **2002**, *99*, 14071.
12. Sinz, M. W. *Ann. Rep. Med. Chem.* **2008**, *43*, 405.
13. The purity of final compounds was determined by HPLC. The final structures are consistent with their ^{1}H NMR and LCMS spectral data. The enantiomeric purity was determined by HPLC and found to be >98% ee.
14. PXR activation relative to percent of control (rifampin) was determined using HepG2 cells transfected with a luciferase reporter construct driven by human PXR cDNA with luciferase activity determined by chemiluminescence.
15. Klapars, A.; Antilla, J. C.; Huang, X.; Buchwald, S. L. *J. Am. Chem. Soc.* **2001**, *123*, 7727.
16. Fraction unbound **1** in mouse plasma = 0.06; fraction unbound **27** in mouse plasma = 0.035 (ultracentrifugation).